EFDA–JET–CP(07)02/04

V. Pericoli-Ridolfini, P. de Vries, J. Mailloux, B. Alper, Y. Andrew, Yu. Baranov, M. Beurskens, P. Beaumont, M. Brix, P. Buratti, G. Calabr, R. Castaldo, R. Cesario, C.D. Challis, V. Cocilovo, K. Crombe, C. Giroud, M. Gryaznevich, T.C. Hender, D. Howell, P. Lomas, M.L. Mayoral, D.C. McDonald, I. Monakhov, S. Nielsen, F. Orsitto, S. Sharapov, P. Smeulders, C. Sozzi, I. Voitsekovitch, K.D. Zastrow, O. Zimmermann, V. Zoita and JET-EFDA contributors

Internal Transport Barrier Studies on JET in ITER-like Plasmas in View of a Steady State Operation

Internal Transport Barrier Studies on JET in ITER-like Plasmas in View of a Steady State Operation

V. Pericoli-Ridolfini[1], P. de Vries[2], J. Mailloux[2], B. Alper[2], Y. Andrew[2], Yu. Baranov[2], M. Beurskens[2], P. Beaumont[2], M. Brix[2], P. Buratti[1], G. CalabrÚ[1], R. Castaldo[1], R. Cesario[1], C.D. Challis[2], V. Cocilovo[1], K. Crombe[3], C. Giroud[2], M. Gryaznevich[2], T.C. Hender[2], D. Howell[2], P. Lomas[2], M.L. Mayoral[2], D.C. McDonald[2], I. Monakhov[2], S. Nielsen[4], F. Orsitto[1], S. Sharapov[2], P. Smeulders[1], C. Sozzi[5], I. Voitsekovitch[2], K.D. Zastrow[2], O. Zimmermann[6], V. Zoita[7] and JET-EFDA contributors[*]

[1]*Associazione Euratom-ENEA sulla Fusione, C. R. Frascati, C.P. 65, 00044-Frascati, Italy*
[2]*Euratom/UKAEA Fusion Association, Culham Science Centre, Abingdon, OX14 3DB, UK*
[3]*Department of Applied Physics, Ghent University, Rozier 44, B-9000 Gent, Belgium*
[4]*Association EuratomRiso, Riso National Laboratory, Roskilde, Denmark*
[5]*Associazione EURATOM-ENEA, IFP-CNR, Via R. Cozzi, 53 - 20125 Milano, Italy*
[6]*Assoziationen Euratom-Forschungszentrum J¸lich, D- 52425, J¸lich, Germany*
[7]*MEdC, Ministry of Education and Research, Bucarest, Romania*
** See annex of M.L. Watkins et al, "Overview of JET Results ", (Proc. 21st IAEA Fusion Energy Conference, Chengdu, China (2006)).*

Preprint of Paper to be submitted for publication in Proceedings of the 5th IAEA TM on Steady State Operation of Magnetic Fusion Devices, (Daejeon, Republic of Korea 14th - 17th May 2007)

1. INTRODUCTION

The steady-state operation of future fusion devices based on the tokamak concept will require the whole toroidal current to be driven non-inductively, via both the bootstrap current mechanism and by means of external power sources. For this purpose then low plasma currents, I_p, would be preferred, in contrast with the need of maintaining a high global energy confinement, which scales almost linearly with I_p, according to the presently accepted scalings. This dichotomy could be solved if the confinement were improved with respect to the basic reference scenario: I_p could then be reduced without a corresponding loss of confinement. The I_p decrease would in turn increase the fraction of the bootstrap current, I_{bs}, being $I_{bs}/I_p \approx \varepsilon^{0.5}\beta_p \propto I_p^{-2}$, where $\varepsilon = a/R$ is the inverse aspect ratio (a, R = minor, major plasma radius) and $\beta_p = 2\mu_0 <p>/<B_{pa}>^2$ is the poloidal beta (μ_0 = vacuum magnetic permeability, <p> = average plasma pressure, $<B_{pa}>$ = average poloidal field magnitude at the plasma boundary).

Possible candidates for such advanced scenarios are regimes with Internal Transport Barriers (ITB) that have been a focus of attention for several years. Indeed, the barrier not only improves the energy confinement, but increases also I_{bs} because of the associated stronger radial pressure gradients. Despite the wide progress made in this field, well reviewed in Ref. [1], many aspects remain either to be investigated or to be optimized for qualifying the ITBs as a valid and reliable advanced scenario for a steady fusion reactor. The most stringent requests come from the need for a high normalized beta, $\beta_N = \beta_T \cdot B_T/(I_p/a)$ ($\beta_T = 2\mu_0 <p>/B^2_T$), and for a high plasma density, both needed for economic attractiveness of a fusion reactor. Moreover, a steady state requires consistency of the radial profile of the non-inductive current, bootstrap plus that driven by external sources, with the current profile required to maintain the ITB itself, both in terms of the local transport reduction and Magneto-HydroDynamic (MHD) stability. These latter points are very difficult to fulfill unless the ITB extends from the plasma centre beyond half the minor radius and if it is not too strong. Indeed, narrow ITBs do not enhance greatly the global confinement, being bounded to a small fraction of the plasma volume, while strong ITBs can easily trigger MHD instabilities (pressure driven kink modes) already at quite low β_N = values ($\beta_N < 2$). In addition, strong ITBs display quite localized I_{bs} profiles that do not meet the requirement for broad current profile of the ITER steady state scenario. Moreover, a 'current hole' magnetic configuration, not suitable for the fusion a-particle confinement, can be easily formed and accumulation of impurities in the centre is favored. The optimal properties of an ITB profile, wide radius and moderate strength, are defined and discussed in Refs. [2, 3].

As a reference for the worldwide research on this topic an advanced steady scenario has been outlined for ITER where the fusion performance is still acceptable, with a power amplification factor Q = 5. The following requirements should be fulfilled: i) confinement enhanced by 50% over the standard H-mode scenario scaling ITER98(y,2) [4], $H_{98y,2} \sim 1.5$, ii) line averaged density $n_e \sim 0.8 \cdot n_{GW}$, with $n_{GW} = I_p/(\pi a^2)$ [10^{20} m^{-3}, MA, m^2]) the Greenwald density [5], iii) $I_{bs}/I_p \geq 0.5$, iv) $\beta_N \sim 3$, v) ITB minor radius $r_{ITB}/a > 0.5$. The value of the plasma safety factor q at 95% of the poloidal flux is $q_{95} \sim 5$. A further condition is that the current profiles should still ensure an

acceptable confinement of the fusion-produced fast particles, i.e. a large region with little of no current density in the plasma core should be avoided.

In this context time has been devoted during the 2006-7 JET experimental campaigns to study and develop such plasmas in an ITER-like configuration, namely with high triangularity, d~0.4. This has been possible only after refurbishing the divertor layout in order to allow those tiles preferentially hit by the plasma and energy exhaust in the high triangularity configuration to sustain elevated thermal loads.

The aim of this paper is to describe the initial progresses on this topic at JET, to illustrate the on-going analysis and to outline the still pending questions and problems.

2. EXPERIMENT - THE CHOICE OF PARAMETERS

The JET plasma parameters adopted as a starting point for the investigations are B_T = 2.3T, I_p = 1.5MA, with $q_{95} \sim 5$. The choice of the parameters is an initial compromise between the need of having high confinement, high bootstrap current and acceptable LHCD efficiency. Unfortunately not all of the requirements have been met simultaneously up to now, as detailed below. The external power sources employed are the Neutral Beam Injection (NBI), up to P_{NBI} = 21MW, the Ion Cyclotron Resonance Heating (ICRH) radio frequency, at f_{ICRH} = 37 MHz and up to P_{ICRH} = 7MW in the H-minority heating scheme ($n_H/(n_H+n_D)$ ~5%), and the Lower Hybrid Current Drive (LHCD) radio frequency, at f_{LHCD} = 3.7 GHz, up to P_{LHCD} = 2.5MW. Density has been varied within the range $0.56 \leq \bar{n}_e \leq 0.74 \cdot n_{GW}$ corresponding to $\bar{n}_e = 0.34\text{-}0.45 \cdot 10^{20}$ m^{-3}.

One of the first point has been to choose the most suitable magnetic configuration, in terms of the elongation, position of the X-point and of the strike point in the divertor chamber, as well as of the shape of the plasma with respect to that of the vessel, and to fix accordingly the waveforms of all the additional power systems involved. This has been pursued with the additional criterion of building a transport barrier as similar as possible on both ions (i^+) and electrons (e^-).

The importance of the configuration is quite evident from Fig.1 where we compare the achieved b_N as a function of the total injected power for the two tested configurations up to now. Investigations are on going to see whether the large difference between them come from the different evolution of the edge temperature and density in the early phase of the discharge, due to the different location of the divertor strike point with respect to the pumping throat. At the switch on of the high power phase this could originate different bootstrap current profiles and consequently different dynamics of the discharge. The better performing configuration was that with the strike point closer to the divertor pumping throat that assured a tighter control of the plasma density and made it easier to establish an electron barrier.

Figure 2 shows the enhancement factor $H_{98(y,2)}$ over the scaling ITER98(y,2) of the global energy confinement time as a function of β_N. The best performing plasmas show values of the thermal $H_{98y,2}$ reaching 1.1. It is neglected the contribution of the fast ions generated by NBI, which can be larger than 35% of the thermal energy content. 5-6% higher values could be obtained by considering

that the LHCD power is absorbed in most cases with very low efficiency in the core plasma, as it will be detailed below. Further improvement would be possible when the ICRH power will be deposited more on axis. Indeed for the chosen B_T and the available f_{ICRH} the power delivered collisionally to the electrons by the resonating H minority ions appears to be beyond half radius, external to the transport barrier.

Figures. 3a) and 3b) compare the achieved β_N as a function of the barrier strength and width respectively. Distinction is also made amongst electrons and ions. The ITB strengths are given as the magnitude of the normalized inverse temperature scale lengths $\rho^*_T = \rho_{L,s}/L_T$, where $\rho_{L,s}$ is the Larmor radius of the ions moving at the sound velocity and $L_T = T/(dT/dr)$ refer to either electrons or ions. The threshold value for an ITB is assumed to be $\rho^*_{T,th} = 0.014$, according to Ref. [6]. The b_N values are averaged over 0.2 s at least during the best performing time interval of the discharge. They reach the value of ~2.7 that is quite close to $4 \sim l_i \sim 2.8$ (l_i is the plasma internal inductance), assumed as a reference for the MHD stability (Troyon limit). Values of β_N up to 3, clearly exceeding the $4 \sim l_i$ limit, have been also achieved though transiently.

Preliminary TRANSP modeling indicates that the fraction of I_{bs} exceeds in the best discharges 40%, with 20% of NBI driven current. The fraction of the LH driven current instead is often very low, due to the high density and relatively low magnetic field that impede a good penetration of the LH waves into the core.

Figures 3a) and b) also show that the best performances are achieved when both i^+ and e^- ITBs are present and tend to approach one another in terms of both width and strength. The maximum ITB radii so far obtained are $R_{ITB,i} \sim 3.6$m (r/a~0.65) for ions and $R_{ITB,e} \geq 3.5$m (r/a~0.55) for electrons. As ITB radius is here taken the ITB footprint, namely the radius where $\rho^*_T = \rho^*_{T,th} = 0.014$. Electron ITBs are generally weaker, $\rho^*_{Te} \leq 0.02$, while $\rho^*_{Ti} > 0.03$, probably because the heating schemes used, NBI and ICRH H minority heating, heat predominantly the ions. Figure 4 shows how the central electron temperature T_{e0}, which is tightly linked to the e^-ITB strength, increases with the ICRH power, i.e. with the power delivered into the electron channel. Further analysis will discover the role of the turbulence behavior that could affect differently the two loss channels. In the high β_p configuration T_{e0} is always higher just because an e^-ITB develops. This gives a good prospect for reaching parity between e^- and i^+ITBs as soon as the power delivered to electrons could be raised and also shifted more on axis inside the good confinement region.

Further evidence that the β increase is due to the presence of an ITB rather than to an improved H-mode quality is presented in Fig.5, where we plot β_N versus the ratio of the edge to the central pressure: clearly the best performances are associated to a heavier weight of the centre, i.e. of the ITB region.

3. EXPERIMENT - THE STABILITY

The stability limit of these regimes with respect to most dangerous n = 1 (n = toroidal periodicity number) kink MHD modes is presented in fig.6: the experimental β_N is plotted versus the stability no-

wall limit deduced from the technique of the resonant amplification of an externally imposed n = 1 perturbation to the magnetic field. Data from the present experiment are considered together with those from the experiment on the β_N limit in ITER-like high triangularity plasmas without ITBs. The absence of clear distinction between them suggests that the presence of the pressure gradients associated to the ITBs has little effect on the overall stability, even though a full reliable comparison should be made for identical q(r) profiles. The importance of this latter come from the observation that the achieved b_N increases as the central q(0) decreases for the non-ITB case [7]. The better performances at lower q(0) and the observation of an improved stability as the ITB radius widens [8] indicate the way to be followed in order to further increase b_N.

Up to now steady conditions have been attained only for $\beta_N \leq 2.5$, when either β_N is feedback controlled in real time or slightly depressed by a mild internal MHD activity. Otherwise, a strong n = 1 MHD mode affecting the whole ITB region starts at a certain time. The delay mostly depends on the waveforms of the main heating, which govern the q(r) profile evolution, as clearly indicated by the Motional Stark Effect (MSE) diagnostics, determining when q(r) losses its the optimum shape. In the best-diagnosed discharges the onset of this very extended and strong mode appears to be related to the loss of reversal in the q(r) profile. To maintain stable q(r) more non-inductive current would be necessary. LHCD was the main tool used in these experiments, but the progress was rather poor, as can be inferred from Fig.7 where the time evolution the minimum value of q(r), q_{min}, is compared for two discharges with the LH power, 0.8 and 2.2MW. Despite the large difference in P_{LHCD} the rate at which q_{min} falls is very similar. The different starting level of q_{min} is due to the different timing of the main heating that starts at 2.8s for Pulse No: 70329 and at 3.3s for Pulse No: 70330, in both cases LH power is added this is 1.2 s. The low accessibility of the LH waves to the core plasma for the chosen density and B_T field is the main reason, as confirmed independently by several LH propagation/absorption codes. Experimental confirmations come from the very low level of suprathermal emission detectable in the Electron Cyclotron Emission (ECE) spectra. According to a previous work on JET in such plasmas the effective absorption of the LH power should be as low as 20% inside $r/a \leq 0.85$ [9].

Other ways have been tried to arrest the q-profile evolution, mainly that of acting on the edge condition to either increase the LHCD accessibility or affect the peripheral I_{bs} profile. Despite the limited progress so far on this point, some room for improvement still exists in regulating the recycling through the plasma-wall distance and in optimizing the strike point position in the divertor. Moreover when higher NBI power will be available and the ICRH system will be upgraded we could extend our operational space to higher B_T, and possibly I_p, in order to improve the LHCD accessibility and exploit fully its potential.

4. EXPERIMENT - THE PERFORMANCES

The best performing plasmas are obtained when q profile with negative magnetic shear is formed by optimizing the start time of the high power NBI and ICRH during the I_p ramp-up. Preliminary

analyses indicate that the optimum time is when q_{min} is just above 2.This apparently triggers an ITB at the radius where a little time later q_{min} is =2, that is generally close to half the radius.

Using LHCD early in the discharge can greatly help in this job, especially in shifting more outward the q_{min}=2 radius. With early LHCD it was much easier to build acceptable e^-ITB in terms of both radius, and strength and consequently to obtain the highest b_N. A possible cause is that electron transport is more affected by q(r). The benefit of the LHCD increases with power until the level that originates a strong current central hole with wide double tearing internal reconnection events. These can make faster the current radial distribution and counterbalance the effect of LHCD off-axis deposition.

It is also very important to avoid large ELMs that are not compatible with a wide ITB. ELMs mitigation has been often attained by puffing a mixture of Ne+D_2, but also the level of the recycling has been found to affect ELMs. However this has not yet avoided the onset of strong ELMs when the edge pressure becomes very high. In this case giant ELMs periodically degrade the energy content by more than 10% at the peak values of β_N, limiting the performance. As briefly outlined above, this has been found to happen at the highest values of β_N ($\beta_N \sim 3$) where the contribution of the pedestal energy is very important. It must be further stressed that no MHD activity was triggered in plasmas with the highest b_N, indicating that in those circumstances a promising q(r) profile shape was obtained.

In the following figures, N. 8a) and b), we compare the time evolution of the main quantities for the best performing (Pulse No: 68927) and the longest lasting (Pulse No: 70322) high β_N + ITB discharges. In fig.8a) we focus mainly onto the ITB characteristics, while in 8b) onto the MHD instability and ELMs.

We note (Fig. 8a) how in Pulse No: 68927 the ion ITB is wider and becomes definitely stronger for t > 5.8s. Even for the discharge where the ITBs are terminated by the detrimental n = 1 MHD mode (at 7.9s for Pulse No: 68927) the ITBs are maintained for longer than 17 energy confinement times. For the almost steady discharge (Pulse No: 70322) two partial collapses of the of i^+ITB at 4.7 and 5.8s occur that are linked to the growth of a n = 5 first and then n = 4 mode close to half radius. An e^-ITB is present instead only in the best performing discharge and it is always weaker and narrower than the i^+ITB. In the other one there is only some very short attempt to build an even narrower e^-ITB.

In fig. 8b) instead we note that Pulse No: 70322 has an even prompter rise of β_N that lasts until the first collapse of the i^+ITB at t ~ 4.7s, then the recovery to the previous value lasts until t ~ 5.8s at the second and definitive collapse of the strong i^+ITB phase. The bottom frame shows the ELMs activity: for Pulse No: 68927 the occurrence of some big ELMs limit periodically the β_N growth. These ELMs are preceded and possibly triggered by a modification of the plasma shape: the elongation increases and the vertical plasma-wall distance decreases. A finer control of the plasma shape was not possible at that time to prevent this effect.

The main difference between the two discharges appears to be the different q(r) evolution, as

illustrated in Fig.9, where the two time traces of q_{min} are plotted. The higher q_{min} for Pulse No: 68927 is consistent with a wider shearless region and then with a wider ITB as indicated in Fig.8a. The difference in q(r) profile is confirmed by the MHD burst-like activity shown in the second frame of Fig.8b for t < 7s. This has been recognized as a fishbone that develop close to the q = 2 surface, since the q=1 surface is doubtlessly absent. The fast $T_e(r)$ profile from ECE indicate these radii at $r_{q=2}$~3.52 and ~3.45m for Pulse No's: 68927 and 70322 respectively, consistently with fig.9 and with the establishing an e^-ITB, or with the attempts to do so, as deduced from Fig.8a). The time traces in fig.9 of the two q_{min}'s separate definitely from each other only for $t \geq 5.7$s, well inside the NBI high power phase. The main differences between the two discharges are in the edge conditions, evidenced in the ELM behaviour that could easily change the bootstrap drive in the periphery, and in the total NBI power, ~2MW more in Pulse No: 68927. Also higher are P_{ICRH} for t < 4.7, see Fig.8b) and the effective ion charge, Z_{eff}~4 in Pulse No: 68927, due the use of neon, against Z_{eff} ~ 2.1 in Pulse No: 70322. We suspect however that these latter changes are less important because of the quite off-axis deposition of the ICRH power and of the small fraction of the OH current that can be affected by a change of resistivity.

Unfortunately, when Pulse No: 70322 was run the whole NBI power was not available to check whether a higher steady b_N could be maintained with the optimum q(r) profile, only by increasing P_{NBI}. Also unsolved then is whether the strong ELMs as in Pulse No: 68927 could be avoided by impeding the fast variation of the elongation by which it is preceded, with a finer control of the plasma shape. The algorithm suited for that, called the plasma extreme shape controller, was not available at the time of Pulse No: 68927, while at the time of Pulse No: 70032 was not available the full power.

The MHD activity limiting the β_N growth in Pulse No: 70032 is more clearly seen in the discharge Pulse No: 70330, where again strong T_i gradient develops and the NBI waveform is very equal to Pulse No: 70332. In fig.10 the time traces of the plasma toroidal rotation frequency for the different spatial channels are shown together with that estimated for the rotation of the mode. This latter, shown as a short thick trace starting at the mode onset at 4.7s and truncated at about 5.5s, gives an indication of the spatial location of the mode. As soon as the mode is born the rotation of the core plasma is clearly strongly slowed down. Also visible it is an initial transfer of momentum to the external plasma. The mode is located in the region of the strongest T_i gradient that is depressed consequent to the reduced rotation, as it can be deduced from Fig. 11, where the $T_i(r)$ profile just before the mode onset at 4.65s, during the slowing down phase at 4.8s and at the end of this latter at 5.4s are plotted.

CONCLUSIONS

Significant progress has been made on high β_N scenario with ITBs for ITER, that is the preferred option for a sustainable steady scenario. Potential for further improvement exists from these initial experiments, especially exploiting the future power increase planned for JET. The present results

indicate that with the same q_{95} target, i.e. with the presumably very similar evolution of the q(r) profile and of the plasma shape, a scenario with B_T = 2.6T and I_p = 1.7MA could be attainable with ITBs and high β_N. The higher B_T should assure a much better penetration of the LH waves and an amount of driven current of the order of 0.4MA that should overcompensate the loss of I_{bs} due to the increased I_p. The waveform and timing of the LH power could then be optimised to obtain the best q(r) profile and the real time control of q(r), that makes use primarily of the LHCD power, could be fully exploited. The b_N drop also associated to the larger B_T should be balanced by the improvement of the confinement time, which is almost linear with I_p, and by the increased power. The major questions about the stability of such advanced regimes in ITER-like configurations could then be better investigated, because of the larger current drive capability.

Further motivation to improve the ITB performance in future JET experiments is given by the fact that the H factors so far achieved are slightly below those required for the envisaged ITER non-inductive scenarios. The more reliable way to this goal is to establish electron and ion ITBs, comparable in terms of size and strength are also within the reach of the near term experiments. Indeed with a more central deposition of the ICRH waves and with more power the quality and the extension of the e^-ITB could approach that of the i^+ITB. More help in this sense can derive from a better exploitation of the LHCD at higher B_T, and by optimizing the target plasma. This can be done in a coarse way, simply by changing the target q_{95}, thus affecting the whole q(r) profile and especially the location of the surfaces with rational q values that are so important in the ITB formation, or in a finer way, tailoring at best the waveform of all the additional heating, whose study has not yet been completed. A contribution to this is expected to come also from the optimization of the profile of I_{bs} during the steps that build up the main heating, according to several modeling investigations of the evolution during this crucial phase. Optimization is expected to come from controlling the plasma-wall interaction. The optimisation of the plasma edge is also important to maximise the pedestal contribution.

REFERENCES

[1]. X. Litaudon et al., *Plasma Phys. Control. Fusi*on, **V. 48** (2006), p. A1–A34

[2]. E.J. Doyle et al, *Nucl. Fusion,* **V. 42**, p. 333 (2002)

[3]. T.C. Luce et al.,, Fusion Sci. Technol., **V. 48**, p. 1212

[4]. ITER Physics Expert Group on Confinement et al., *Nucl. Fusion*, **V. 39** (1999)**,** Ch. 2, p 2175-2249

[5]. M.J. Greenwald et al., *Nucl. Fusion*, **V. 28** (1988)**,** p. 2199

[6]. G. Tresset et al., *Nucl. Fusion,* **V. 42** (May 2002), p. 520-526

[7]. M. Gryaznevich, private communication

[8]. L. Lao et al. APS 1999

[9]. V. Pericoli Ridolfini et al., *Plasma Phys. Controll. Fusion,* **V. 39**, p. 1115-1128

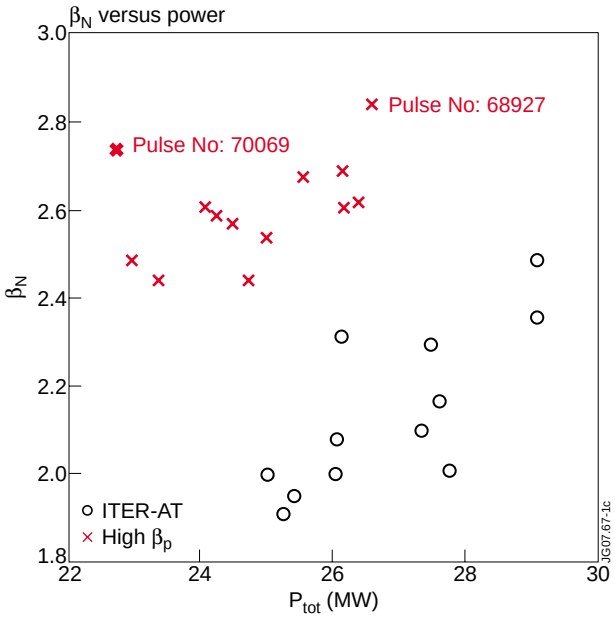

Figure 1: Plot of β_N versus the total injected power. Different symbols refer to the two different plasma configurations used.

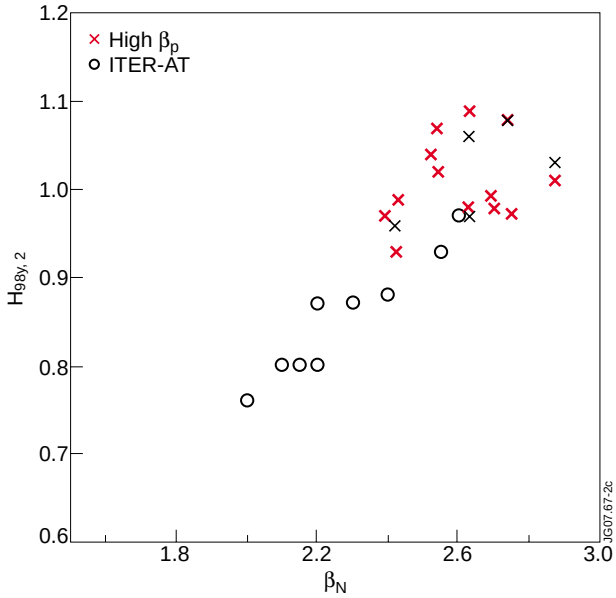

Figure 2: Plot of the enhancement confinement factor over the ITER98(y,2) scaling versus β_N. Different symbols refer to the two different plasma shapes used in the experiment, as indicated in the legend. The energy content minus the fast-ion contribution is considered only. If this latter is considered values $H_{98y,2}>1.5$ are obtained.

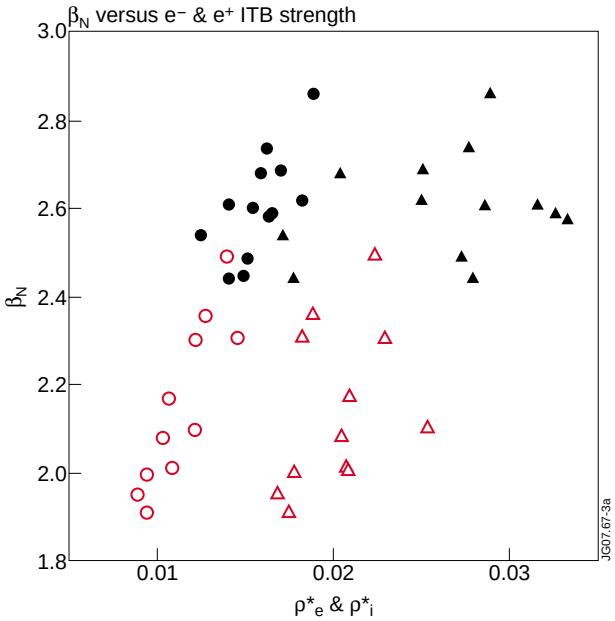

Figure 3(a): Plot of β_N versus the e^- and i^+ ITB strength $r^*_{T(e,i)}$. Circles refer to electrons, triangles to ions; full symbols to high β_p configuration, empty ones to ITER-AT. The highest β_N and ρ^*_T triangles are achieved only with the high β_p configuration.

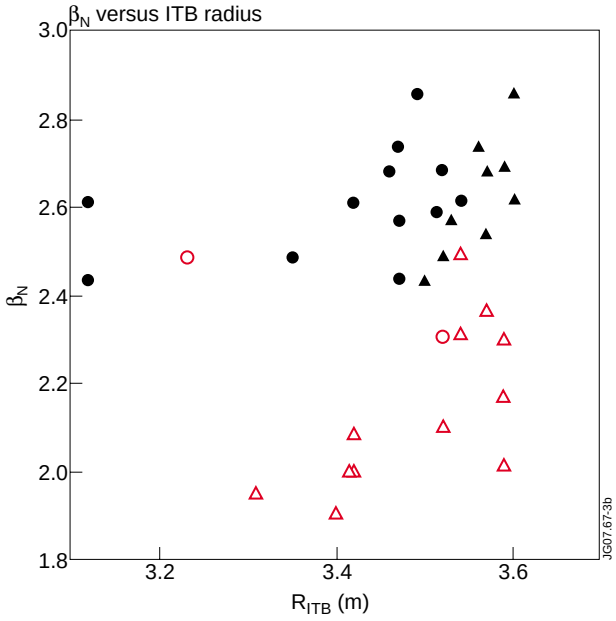

Figure 3(b): Plot of β_N versus the e^- and i^+ ITB radius, given by the condition $\rho^*_T=r^*_{T,th}=0.014$. Circles refer to electrons, triangles to ions; full symbols to high β_p configuration, empty symbols to ITER-AT. e^-ITB are achieved only with the high β_p configuration and on average tend to approach to each other for higher β_N.

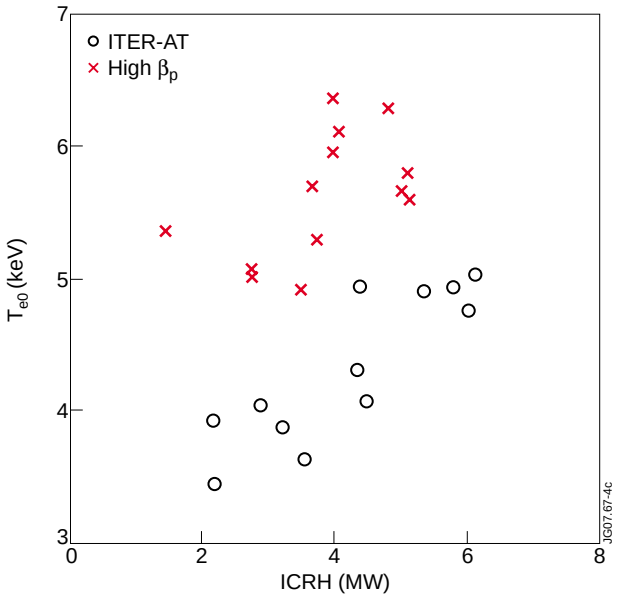

Figure 4: Plot of the central electron temperature versus the ICRH power, for the two plasma configurations used in the experiment, as specified in the legend. The group on the top has developed an e-ITB.

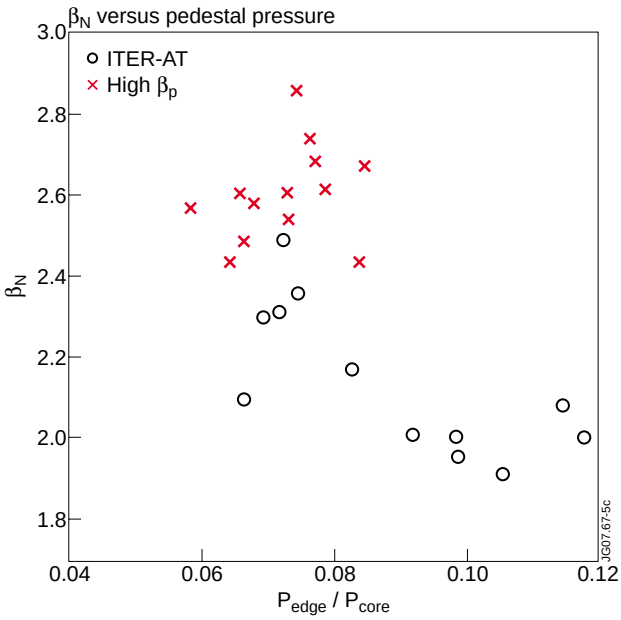

Figure 5: Plot of β_N versus the ratio of the edge pressure to the central pressure. The density values are those along the central and peripheral chord (R=3.75m) of the interferometer. This graph shows how big is the contribution of the core, i.e. of the ITB to the increase of β_N.

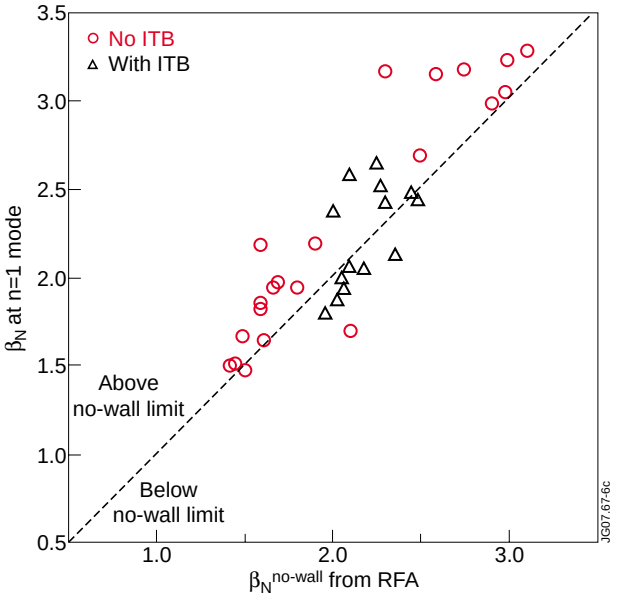

Figure 6: Plot of the achieved β_N versus that calculated as the no-wall limit, from the resonant filed amplification (RFA) technique. Distinction is made, as specified in the legend, between the ITB and no-ITB case.

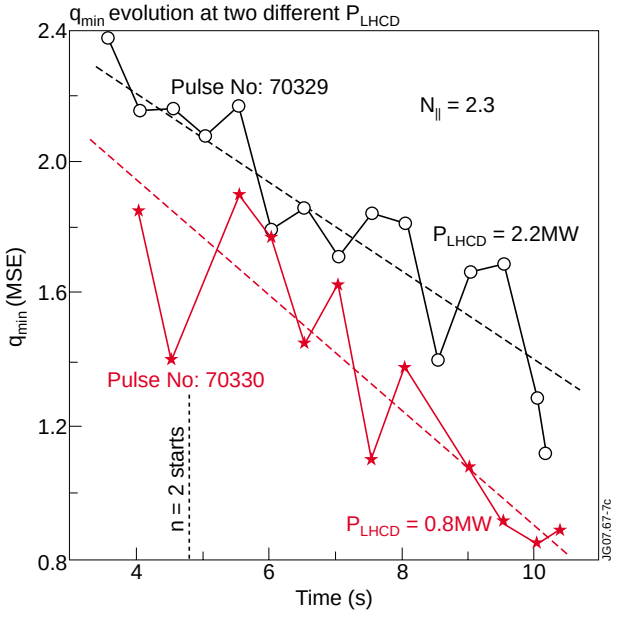

Figure 7: Time evolution of the q_{min} value, according to the MSE diagnostic, for two discharges with different LH power. No significant difference is visible in the rate of decay of q_{min}, indicating a poor effect of the LHCD. In both cases the LH power is added 1.2s after the start on the high heating phase

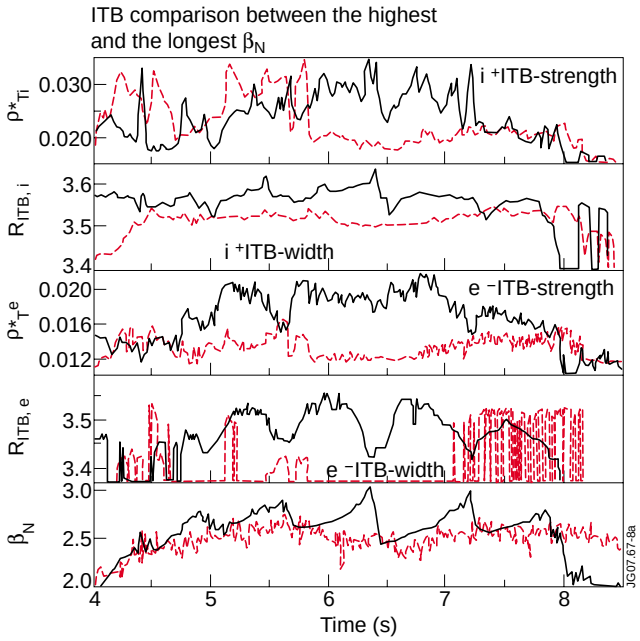

Figure 8 (a): Time traces relevant to the ITBs (ion the top two, electron the following two) for two discharges: that with the highest achieved β_N (Pulse No: 68927 blue trace) and that lasting longest (Pulse No: 70322 red trace).

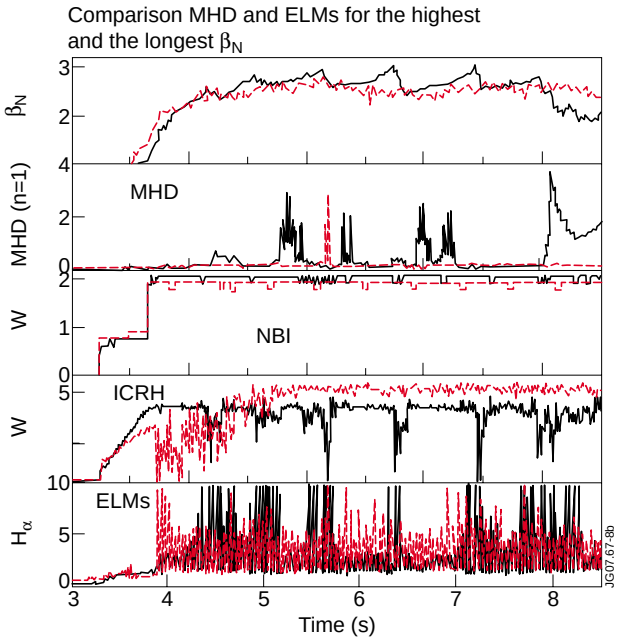

Figure 8(b): Time traces relevant to the MHD instability and ELMs for two discharges: that with the highest achieved β_N (Pulse No: 68927 blue trace) and that lasting longest (Pulse No: 70322 red trace). The high β_N phase is terminated for Pulse No: 68927 by a strong MHD n=1 mode at 7.9 s

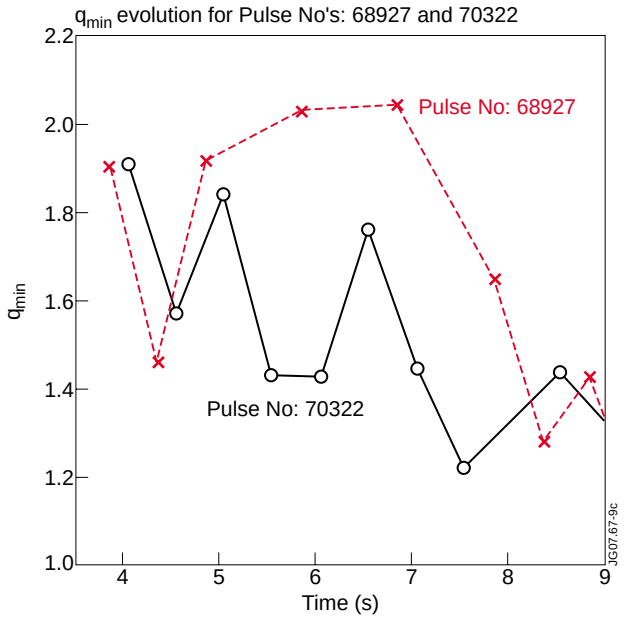

Figure 9: Time evolution of q_{min}, according to MSE diagnostic for the same discharges as in fig. 8. The higher q_{min} that develops in Pulse No: 68927 is most probably due to the large NBI power. It indicates also that the shearless region is wider.

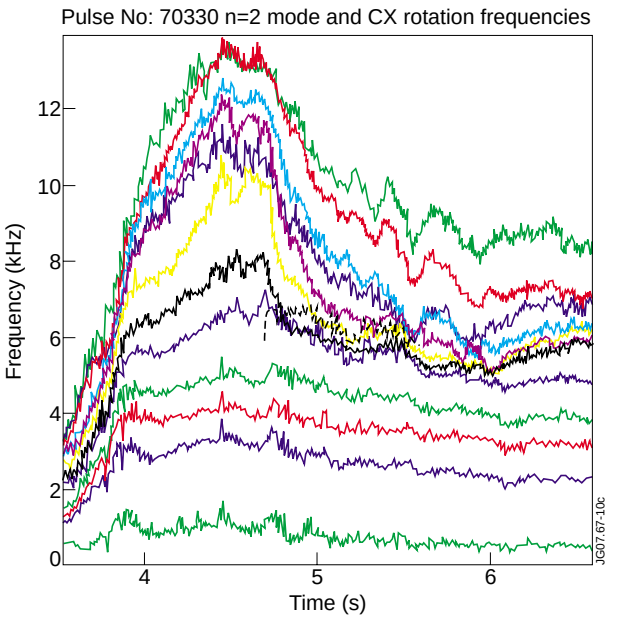

Figure 10: Time traces of the toroidal rotation along the radii of the charge exchange spectroscopy. Rotation increases from periphery to center. The short thick and black curve starting at about 4.7s and ending at 5.5s indicates the estimated rotation speed of the n=2 mode and gives an indication of its spatial location

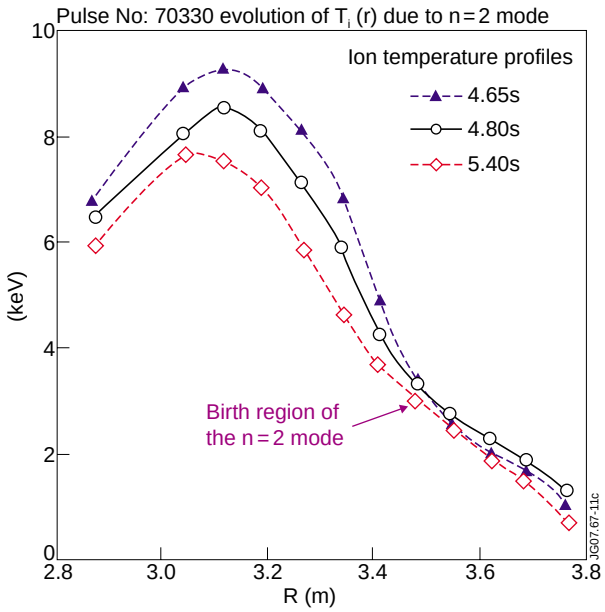

Figure 11: Ion temperature profiles for the same discharge of fig. 10, before the start of the n=2 mode, during the slowing down phase and at the end of this latter. The approximate radial location of the mode is recognized from the radius where the first and second trace cross over to each other at R~3.5 m. the mode transfer some energy and momentum from the core to the periphery